Fluorescence Fluctuation Spectroscopy on Viral-Like Particles Reveals Variable Gag Stoichiometry

Yan Chen,[†¶*] Bin Wu,[†] Karin Musier-Forsyth,[‡] Louis M. Mansky,[§¶] and Joachim D. Mueller[†¶]
[†]School of Physics and Astronomy, University of Minnesota, SE Minneapolis, Minnesota 55455; [‡]Departments of Chemistry and Biochemistry, Ohio State University, Columbus, Ohio 43210; [§]Departments of Diagnostic and Biological Sciences and Microbiology, University of Minnesota, Minneapolis, Minnesota 55455; and [¶]Institute for Molecular Virology, University of Minnesota, Minneapolis, Minnesota 55455

ABSTRACT Fluorescence fluctuation spectroscopy determines the brightness, size, and concentration of fluorescent particles from the intensity bursts generated by individual particles passing through a small observation volume. Brightness provides a measure of the number of fluorescently labeled proteins within a complex and has been used previously to determine the stoichiometry of small oligomers in cells. We extend brightness analysis to large macromolecular protein complexes containing thousands of proteins and determine their stoichiometry. This study investigates viral-like particles (VLP) formed from human immunodeficiency virus type 1 (HIV-1) Gag protein expressed in COS-1 cells using fluorescence fluctuation spectroscopy to determine the stoichiometry of HIV-1 Gag within the particles. Control experiments establish that the stoichiometry and size of VLPs are not influenced by labeling of HIV-1 Gag with a fluorescent protein. The experiments further show that the brightness scales linearly with the amount of labeled Gag within the particle. Brightness analysis shows that the Gag stoichiometry of VLPs formed in COS-1 cells is not constant, but varies with the amount of transfected DNA plasmid. We observed HIV-1 Gag stoichiometries ranging from ~750 to ~2500, whereas the size of the VLPs remains unchanged. This result indicates that large areas of the VLP membrane are void of Gag protein. Therefore, a closed layer of HIV-1 Gag at the membrane is not required for VLP production. This study shows that brightness analysis has the potential to become an important tool for investigating large molecular complexes by providing quantitative information about their size and composition.

INTRODUCTION

Fluorescence fluctuation spectroscopy (FFS) observes the signal fluctuations generated by individual fluorescent particles passing through a small optical observation volume (<1 fL). Statistical analysis of the fluctuations provides information about sample properties (1). The most widely used method, fluorescence correlation spectroscopy (FCS), determines the concentration and temporal properties of proteins from intensity correlation functions (2). Photon counting histogram (PCH) and related techniques extract the brightness and the average particle occupation number within the observation volume from the data (3). The brightness of a molecule is defined as the average fluorescence intensity of a single particle. FCS and brightness analysis are applied both in vitro and inside cells (4–9).

Brightness encodes the stoichiometry of a protein complex. This concept was experimentally verified using green fluorescent protein (GFP) as a marker and has been applied to study the concentration-dependent dimerization of nuclear receptors in living cells (10). Brightness analysis was subsequently generalized to characterize the stoichiometry of heteroprotein complexes by labeling with differently colored fluorescent proteins (11,12). Thus far, brightness analysis has been carried out on oligomers containing only a few labeled proteins. W probe the stoichiometry of the human immunodeficiency virus type-1 (HIV-1) Gag (group specific antigen) polyprotein within viral-like particles. These particles contain hundreds to thousands of labeled Gag molecules and represent a significantly more complex system than previous applications of this technique.

Gag is crucial for the assembly of the HIV-1 virus. Experiments have shown that expressing Gag in cells in the absence of other viral proteins is sufficient for the production and release of viral-like particles (VLP) with the same size as authentic viral particles (13,14). Because VLPs are easy to generate, are noninfectious and much simpler in composition than the viruses, they constitute a model system for the study of viral assembly. VLPs are enveloped by a lipid membrane that the particle acquires from the host cells in the budding process. During budding, a small vesicle (~140 nm diameter) with Gag bound at the membrane is formed and released into the extracellular medium. The stoichiometry or copy number of Gag molecules residing on a single VLP or virion has been the subject of numerous studies. The reported values vary considerable, ranging from ~1000 to ~5000 (15–21). In this study, we use fluorescence fluctuation spectroscopy (FFS) to investigate the stoichiometry of Gag in VLPs formed by HIV-1 Gag protein expressed in COS-1 cells.

The results of this study provide a plausible explanation for the different HIV-1 Gag stoichiometries reported in the literature. Our data also show that the formation of a closed self-assembled layer of Gag is not required for VLP formation by cells, and establish the utility of brightness analysis as a tool to gain quantitative information regarding the assembly of complex macromolecular structures.

Submitted April 28, 2008, and accepted for publication October 9, 2008.

*Correspondence: chen@physics.umn.edu

Editor: Elliot L. Elson.

0006-3495/09/03/1961/9 $2.00

doi: 10.1016/j.bpj.2008.10.067

MATERIAL AND METHODS

Experimental setup

Two-photon excitation with a Ti:sapphire laser was carried out at a wavelength of 960 nm on a modified two-photon microscope as described earlier (10). The viral particles are measured using a 63X Plan Apochromat oil immersion objective (N.A. = 1.4) with an excitation power of <0.3 mW. FFS data are acquired at sampling frequencies ranging from 20 to 200 kHz and recorded for further analysis.

Expression vector and sample preparations

Gag^{YFP} vector (22) is a kind gift from Dr. Paul Spearman (Emory University). Cos-1 cells, obtained from ATCC (Manassas, VA), were maintained in 10% fetal bovine serum and DMEM (without phenol red). Transfections were carried out with transfectin according to manufacturer's protocol (BioRad, Hercules, CA). Cells were kept at ~70% confluency on the day of transfection. For a typical viral particle experiment, 0.3 μg of vector is diluted and mixed with 0.5 μL of transfectin. The transfection complex is added to a cell culture plate with a growth area of 10 cm^2. After 24 h post-transfection, cell medium is collected and spun at 12,000 $\times$ g for 2 min. Concentrated HEPES buffer was immediately added to the supernatant to a final concentration of 25 mM. The VLPs are either concentrated with a Centricon filter at 16,000 $\times$ g or purified by centrifugation at 40,000 $\times$ g for 2 h through sucrose cushion. A volume of 200 μL of VLP solution was added to an 8-well Nunc Lab-Tek Chamber Slide (Thermo Fisher Scientific, Pittsburgh, PA) and mounted on the two-photon microscope. A lid was placed on the chamber slide to eliminate sample loss by evaporation.

FFS data analysis

The autocorrelation function calculated from the data is fit to a single species diffusion model with a 3D-Gaussian point spread function to determine the diffusion time τ_D (1). According to the Stokes-Einstein relation, the ratio of the diffusion time of two samples is equal to the ratio of the hydrodynamic radii of the diffusing particles, $\tau_{D1}/\tau_{D2} = r_1/r_2$. The measured diffusion time of fluorescent spheres with a radius of 0.025 μm was used to calculate the average diameter of the VLPs. The PCH function is calculated from the FFS data. A single species is defined in PCH by its brightness ε and the average number N of particles in the optical observation volume (3). Deadtime and afterpulsing corrections have been applied as described previously (23). If the molecular brightness contrast is sufficient, PCH analysis successfully resolves a mixture of species without any additional information about the sample (24). Fitting of PCH was carried out by programs written in IDL (Research Systems, Boulder, CO). Error analysis of FFS experiments has been carried out as described previously (24).

FFS brightness calibrations

All experiments are conducted in a power range where the fluorescence intensity of YFP squares quadratically with the excitation power to ensure the absence of unwanted optical effects. It was also confirmed that under these conditions the brightness of YFP scales quadratically with excitation power, whereas the average particle number N remained constant. These results confirm that the observation volume is constant. At the low excitation powers used for most VLP measurements long data acquisition times are required for an accurate determination of the brightness and particle number of YFP. Thus, to shorten the data acquisition time the brightness ε_{YFP} of YFP was determined by $\varepsilon_{YFP} = I_{low}/N_{high}$, where I_{low} is the intensity measured at low power, whereas N_{high} is the particle number determined from a measurement at a higher power.

The data acquisition time was chosen so that each FFS experiment records at least 1000 VLPs traversing the observation volume to record a sufficient number of fluctuations for statistical analysis of the data. VLPs are much brighter than individual YFP molecules. To rule out the presence of saturation or other unwanted optical effects FFS experiments are carried out on a VLP sample as a function of excitation power. The brightness per particle and the average particle density was investigated over the power range from 0.1 mW to 0.7 mW by PCH analysis. To compensate for the loss of fluorescence signal at lower excitation powers we progressively increased the data acquisition time from 30 min to 2 h to acquire sufficient statistics for accurate analysis of the fluctuation data.

Determination of stoichiometry by brightness analysis relies on a well-behaved fluorescent protein. We show in the Supporting Material that YFP is suitable for quantitative brightness experiments.

Other data analysis

TEM studies were carried out on a Jeol JEM 1200-EX II microscope (Jeol Ltd., Tokyo Japan). Purified viral samples are prepared and positively stained using methanolic uranyl acetate (25). Viral samples were examined by TEM at an accelerating voltage of 80 kV. Images were analyzed by software written in IDL.

The SDS-PAGE gel is stained by SYPRO ruby protein gel stain and imaged with a GE Typhoon Scanner. The integrated intensities F_{Gag} and F_{GagYFP} of the Gag and Gag^{YFP} bands are determined with software written in IDL, which also corrects for the fluorescence background of the gel. The fractional intensity $\tilde{x} = F_{GagYFP}/(F_{Gag} + F_{GagYFP})$ is equal to the mole fraction x of labeled Gag in the VLP sample, if Gag and Gag^{YFP} stain identically. However, because the staining of the two proteins potentially differs, the fractional intensity is only an approximate measure of the mole fraction of labeled Gag.

RESULTS

Fluorescence fluctuation experiments were carried out on VLPs prepared with yellow fluorescent protein (YFP) -tagged HIV-1 Gag (22) expressed in COS-1 cells. A typical fluorescence intensity trace is shown in Fig. 1 *A*. As evident from this plot, the fluorescence intensity exhibits discrete intensity spikes as a function of time. The intensity spikes indicate very bright, but rare fluorescent particles diffusing through the small two-photon excitation volume. The amplitude of the spike intensity varies, reflecting the stochastic nature of the diffusion path through the inhomogeneously illuminated excitation volume. A particle passing through the center of the volume ignites a much stronger burst of photons than if the particle passes along the edge of the volume. The probability distribution of the recorded photon counts is shown in Fig. 1 *B* (*square symbols*). Photon counting histogram (PCH) analysis was carried out on the probability distribution to determine both the brightness ε and the average number of particles in the optical observation volume (3). For a complex with brightness ε that contains r proteins labeled with the fluorescent protein YFP, it is useful to introduce the normalized brightness b as the ratio of the brightness ε of the protein complex to the brightness ε_{YFP} of monomeric YFP, $b = \varepsilon/\varepsilon_{YFP}$ (12). Because brightness scales with the number of fluorescent proteins in the complex, the normalized brightness is a measure of the stoichiometry r of the labeled protein within the complex, $r = b$ (10,11).

A two-species model describes the experimental PCH (reduced $\chi^2 = 1.6$). A χ^2 test with a significance level of

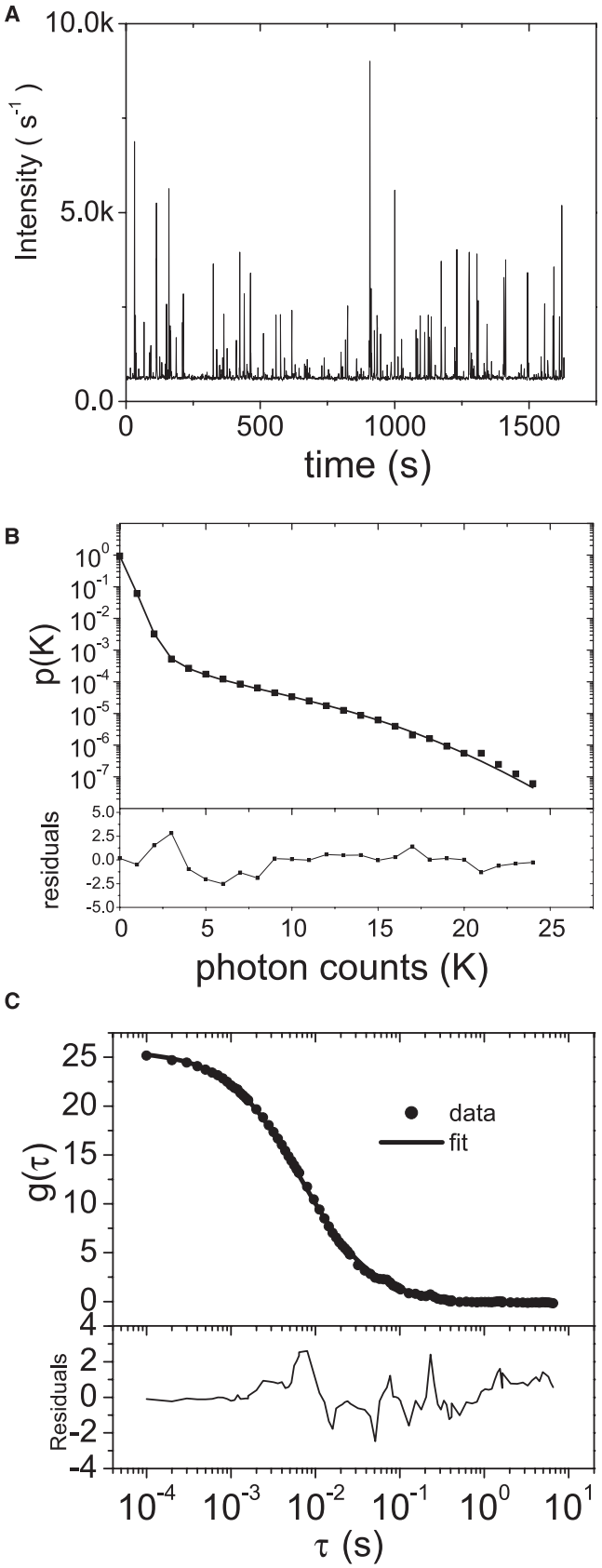

5% shows that an additional brightness species is not warranted. In fact, if the data are fit to a model including an extra brightness species, its parameters are not well-defined as judged by a *t*-test. The photon count distribution of the first species is well approximated by a Poissonian with an intensity of 580 counts per second. The Poisson distribution indicates that the first species consists of many dim molecules with a brightness close to zero. This fluorescent species represents the autofluorescence background of the sample as confirmed by a measurement of a sample prepared without viral particles. PCH analysis identifies this background in every VLP sample measured. For simplicity, we will not report this background in the remainder of the article. The other species with a brightness of 330,000 s^{-1} and a particle density of 5×10^{-4} particles per excitation volume defines the VLPs. This value of the brightness is 750 times higher than that of monomeric YFP under identical experimental conditions. The normalized brightness of $b = 750$ indicates that a viral particle contains on average 750 copies of Gag^{YFP}.

The same raw data were also analyzed by fluorescence correlation spectroscopy. The autocorrelation function of the data is shown in Fig. 1 *C* together with a fit to a single species diffusion model with a diffusion time of 7.6 ms. A single species fit is sufficient, because the autofluorescent background is too weak to affect the fluctuation amplitude of the autocorrelation function. The diffusion time translates into a hydrodynamic diameter of 130 nm for the viral particles.

The presence of undesired optical effects such as saturation and bleaching affect autocorrelation and PCH analysis and result in a biased interpretation of the data. To exclude such a bias, we carried out FFS measurements on a VLP sample as a function of excitation power. The particle density and the brightness per particle are shown in Fig. 2, *A* and *B*, respectively, as a function of excitation power. Because the excitation volume is power independent in the absence of bleaching and saturation, the number of VLPs within the excitation volume should be power independent, as confirmed by the data in Fig. 2 *A*. Molecular brightness of the particles, on the other hand, depends on the excitation power. A fit of the data to a power law yields a power dependence of 1.98, which agrees with the expected quadratic power dependence of molecular brightness in the absence of bleaching and saturation.

Tagging Gag with YFP could potentially interfere with the assembly of VLPs. To rule out such complications, a number of control experiments were carried out. We refer to particles containing labeled protein as Gag^{YFP} VLPs, whereas unlabeled particles are denoted as Gag VLPs. We first compared

FIGURE 1 FFS data for a VLP sample. (*A*) Fluorescence intensity time trace. (*B*) PCH data (*diamonds*) and fit (*solid line*) to a two species model. The first species is very dim with a brightness equal to that of a control sample void of VLPs. The second, bright species has a normalized brightness of ~750. (*C*) A fit of the autocorrelation function determined a hydrodynamic diameter of 130 nm.

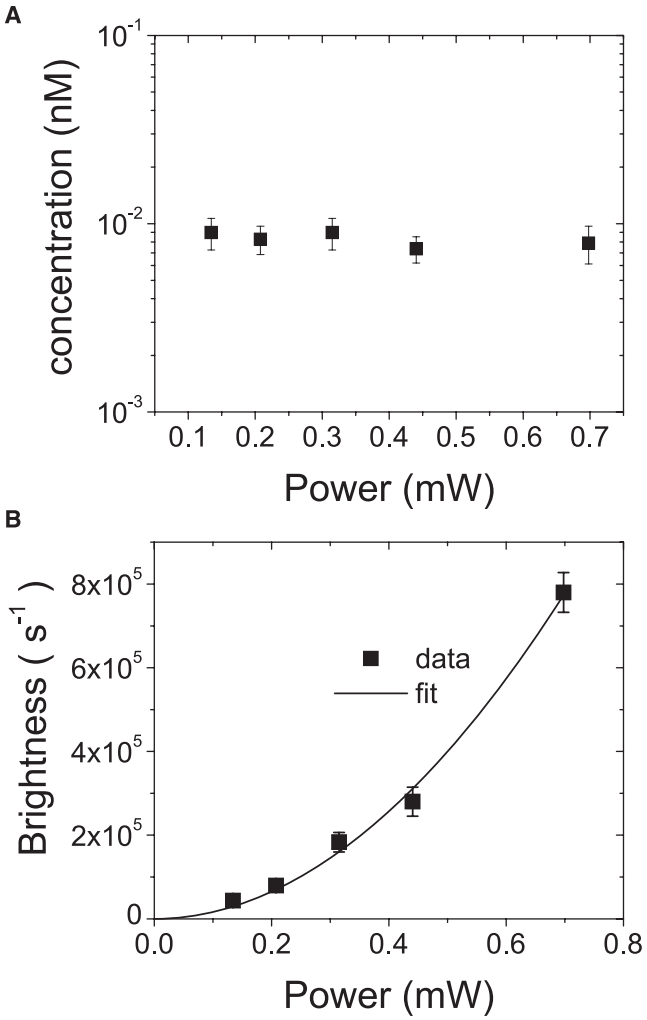

FIGURE 2 Power dependence of a VLP sample. (*A*) The concentration is shown as a function of excitation power. PCH analysis determined the average particle number N in the observation volume, which was converted into a concentration by dividing by the observation volume. (*B*) The brightness determined by PCH analysis is shown as a function of excitation power together with a fit to a power law. The fitted exponent of 1.98 agrees within error with the expected quadratic power-law dependence.

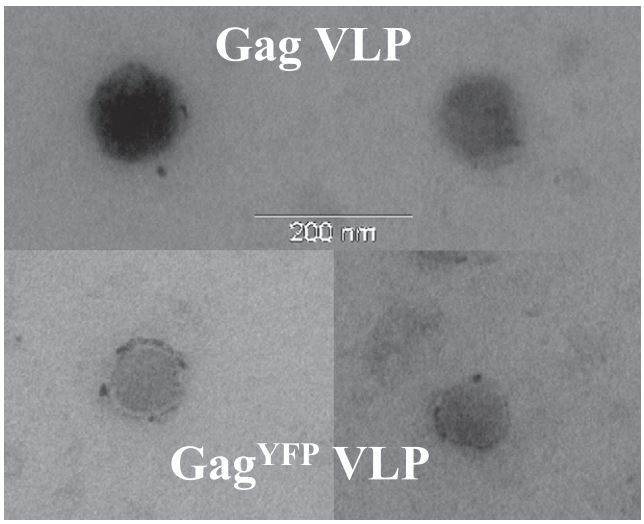

FIGURE 3 Positively-stained transmission electron micrograph of VLP samples. Two Gag VLP particles are shown on top of the figure, whereas the bottom depicts two Gag^{YFP} VLP particles. Image analysis of 66 stained Gag VLP particles determined an average diameter of 129 ± 12 nm. Analysis of 33 Gag^{YFP} VLP particles identified an average diameter of 130 ± 17 nm.

the size of fluorescently tagged and untagged VLPs with transmission electron microscopy (TEM). Images of positively stained VLPs are shown in Fig. 3. Although the two samples stain differently, the images show a spherical cross section for both cases. Image analysis of stained Gag VLPs provides an average diameter of 129 ± 12 nm ($n = 66$), whereas the average diameter of Gag^{YFP} VLPs is 130 ± 17 nm ($n = 33$). We conclude that VLPs formed with Gag and Gag^{YFP} have the same average size and shape.

For the next set of control experiments, cells were cotransfected with a mixture of Gag and Gag^{YFP} plasmid. The Gag/Gag^{YFP} VLPs harvested from cotransfected cells will simultaneously carry Gag and Gag^{YFP}. If labeling of Gag with YFP does not interfere with assembly, then Gag and Gag^{YFP} will be incorporated into the particle without preference. In other words, the composition of Gag and Gag^{YFP} in the VLPs will reflect the relative concentration of these proteins within the cell. Conversely, if Gag^{YFP} negatively interferes with assembly, we expect that viral particles will preferentially incorporate Gag over Gag^{YFP}, which will lead to VLPs enriched in Gag compared to its cellular concentration.

To vary the cellular concentration ratio of labeled and unlabeled Gag, cells were transfected with different plasmid mixtures of Gag/Gag^{YFP}. An assumption was made that the composition of the plasmid mixture also determines the relative amount of expressed protein. If labeling does not affect assembly, then the mole fraction x of labeled Gag protein found in the particle should match the mole fraction y of labeled plasmid. In contrast, if labeling interferes with particle assembly, the mole fraction of labeled protein is not linearly correlated with the mole fraction of labeled plasmid.

The normalized brightness $b(x)$ of a Gag/Gag^{YFP} VLP sample with a Gag^{YFP} mole fraction x is given by $b(1)x$, where $b(1)$ is the normalized brightness of pure Gag^{YFP} VLPs. Note that this relationship also requires that the total stoichiometry of labeled and unlabeled Gag in the VLP is independent of the composition of the plasmid mixture. For example, if labeling does not affect assembly, the VLPs formed in cells transfected with a 1:1 mixture of Gag and Gag^{YFP} ($y = 0.5$) are expected to carry equal amounts of Gag and Gag^{YFP} ($x = 0.5$). The brightness of the VLP sample is reduced, because only half of the Gag proteins are fluorescent. If the total Gag stoichiometry is 750, the copy number of Gag^{YFP} is 375, which results in a normalized brightness of $b(0.5) = 375$.

Individual VLP samples were prepared by transfecting cells with specific mole fractions of Gag^{YFP}/Gag plasmid.

The brightness of the collected and concentrated viral particles was measured for each sample. Fig. 4 shows the normalized brightness of Gag/Gag^{YFP} VLP samples as a function of the mole fraction y of labeled Gag plasmid used for transfection. As expected, the normalized brightness or Gag^{YFP} copy number is reduced with decreasing mole fraction of the Gag^{YFP} plasmid. The solid line in Fig. 4 is a fit of the data to the linear function, $b(y) = b(1)\ y$, confirming that the Gag^{YFP} copy number $b(y)$ scales linearly with the mole fraction of labeled Gag plasmid. This experiment was repeated two times with identical outcomes. The linear relationship between the Gag^{YFP} copy number of the VLPs and the mole fraction of labeled Gag plasmid supports the assumption that Gag^{YFP} does not alter the stoichiometry of the viral particle.

To further support this result, we carried out an independent biochemical assay on VLP samples by separating Gag and Gag^{YFP} via denaturing polyacrylamide gel electrophoresis. Viral particles were collected from cells cotransfected with different Gag^{YFP} and Gag plasmid mixtures, concentrated and loaded onto a denaturing gel. The gel was fluorescently stained and imaged (Fig. 5 *A*). The two bands corresponding to Gag and Gag^{YFP} were clearly separated and the integrated intensity of each band was quantified by image analysis. Using these values, the fractional intensity $\tilde{x}$ of the Gag^{YFP} band relative to the total intensity of the two Gag bands was determined. The fractional intensity is an approximate measure of the mole fraction x of labeled Gag in the VLP sample. Fig. 5 *B* displays the calculated fractional intensity as a function of the mole fraction y of the labeled Gag plasmid used for transfection. The data show that the fractional intensity $\tilde{x}$ not only scales linearly with the mole fraction y of labeled Gag plasmid, but that both values are approximately the same, as illustrated by the solid line $\tilde{x} = y$. In other words, the mole fraction of labeled protein within VLPs is equal to the labeled plasmid mole fraction. This result confirms that no preference of packaging Gag over Gag^{YFP} exists.

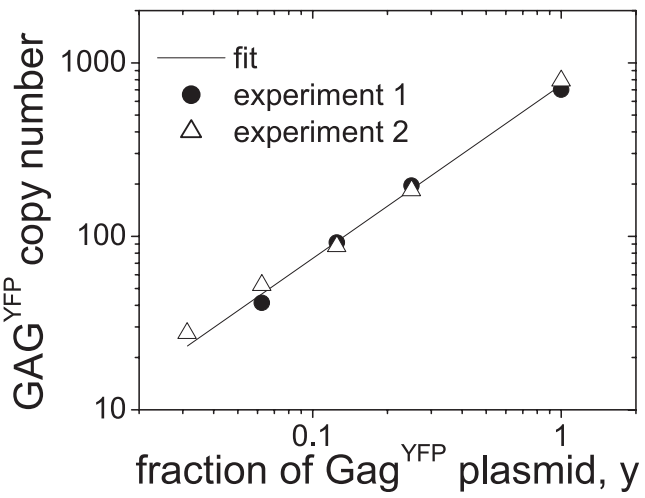

FIGURE 4 Stoichiometry of Gag^{YFP} in the presence of unlabeled Gag. VLPs produced from cells cotransfected with Gag^{YFP} and Gag plasmid. The Gag^{YFP} copy number is shown as a function of mole fraction of labeled Gag plasmid. The graph shows two sets of independent measurements. A linear fit to the function $b(y) = b(1)\ y$ with $b(1) = 750$ is shown as a solid line.

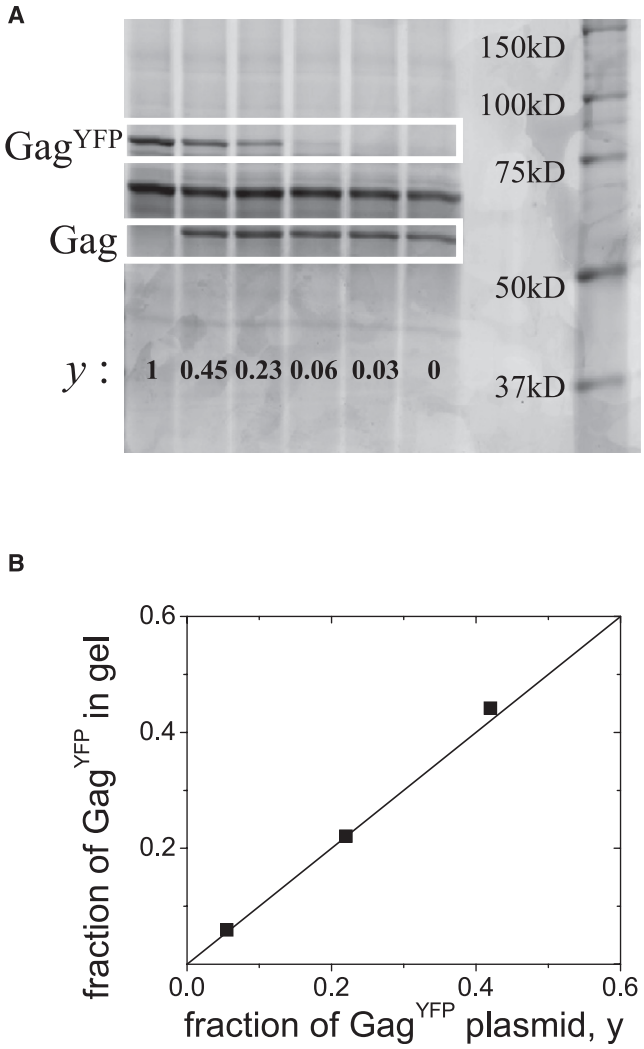

FIGURE 5 SDS-PAGE gel (12.5%) of VLP samples containing Gag^{YFP} and Gag. (*A*) The mole fraction of labeled Gag plasmid is indicated at the bottom of each lane. The bands are fluorescently stained with SYPRO ruby protein gel stain and imaged. Two bands with positions that agree with the molecular weights of Gag and Gag^{YFP} are present (*bottom band*: Gag; *top band*: Gag^{YFP}; *middle band*: BSA from the cell medium). (*B*) Mole fraction of Gag^{YFP} in VLPs containing a mixture of Gag^{YFP} and Gag, as established by quantitation of bands on a denaturing polyacrylamide gel. The graph displays the mole fraction of Gag^{YFP} protein as a function of the mole fraction of labeled Gag plasmid used for cell transfection. The line through the origin with a slope of one illustrates the linear relationship between the protein mole fraction and the plasmid mole fraction.

We also determined the autocorrelation function of each mixed Gag/Gag^{YFP} VLP sample. This analysis showed that the diffusion time of the particle is unchanged within experimental uncertainty. This result shows that the size of the

TABLE 1 FFS analysis of VLP samples prepared by transfection with different amounts of DNA

	Brightness species 1		Brightness species 2		
Plasmid (μg)	Gag copies	N	Gag copies	N	Diameter (nm)
0.15	750 ± 40	(8.1 ± 0.4) 10^{-4}			130 ± 24
0.60	1200 ± 150	(4.1 ± 0.6) 10^{-4}	1600 ± 240	(1.5 ± 0.8) 10^{-4}	130 ± 18
0.90	1300 ± 140	(6.7 ± 0.7) 10^{-4}	2500 ± 220	(1.5 ± 0.4) 10^{-4}	130 ± 20

PCH analysis identified two brightness species for transfection with 0.60 μg and 0.90 μg of plasmid. N is the average number of particles in the optical observation volume. The hydrodynamic diameter was determined from the autocorrelation function.

particles is independent of the Gag/Gag^{YFP} composition of the VLP sample.

PCH analysis of all VLP samples reported thus far identified a single brightness species associated with the particles. Furthermore, all fluorescence fluctuation experiments point to a stoichiometry of ~750 Gag proteins per particle. In these initial experiments, the total amount of DNA used for transfection (0.15 μg) was kept constant. To determine whether the brightness properties of VLPs depend on the transfection conditions, we carried out a series of experiments wherein we transfected COS-1 cells with different amounts of DNA. Several identical cell plates were transfected with varying amounts of DNA plasmid, while keeping the amount of transfection reagent constant. Supernatant from the individual cell plates was collected and measured. The results of the brightness analysis are reported in Table 1. Interestingly, a single VLP brightness species failed to describe the data when higher plasmid amounts were used and therefore, a second species was included in the analysis. The normalized brightness was calculated to determine the Gag^{YFP} copy number.

For the lowest amount of DNA transfection (0.15 μg), the VLP sample is described by a single brightness species with a stoichiometry of 750 copies of Gag per viral particle. Cells transfected with 0.60 μg of DNA produced VLPs described by two brightness species with stoichiometries of 1200 and 1600 copies of Gag per VLP. Transfection with 0.9 μg of DNA resulted in two species with stoichiometries of 1300 and 2500 copies of Gag per particle. The data show that raising the amount of transfected DNA results in an increase of the Gag stoichiometry.

The autocorrelation function of each sample was calculated from the same data used for PCH analysis. In all cases, a single diffusing species described the correlation functions. The hydrodynamic diameter of the VLPs, which was calculated from the fitted diffusion time, is reported in Table 1. The results indicate that the hydrodynamic size of the VLPs is independent of the amount of transfected DNA.

DISCUSSION

The experiments on VLPs carried out in this study established that FFS provides quantitative information about the size and composition of large supramolecular complexes. The brightness of these particles, which contain hundreds to thousands of labeled proteins, is much larger than that of the monomeric protein. To ensure a meaningful comparison between the different experiments, we verified that all FFS parameters are well-behaved over the relevant range of excitation powers. The brightness of VLPs scales quadratically with power, whereas the diffusion time and the observation volume are power independent. This result also confirms that optical trapping of the VLPs by the laser beam is not occurring. Another potential concern is the finite size of the particles, because FFS theory assumes point particles. To determine the effect of size on brightness we use a theory that accounts for the finite size of particles (26). The same method as presented for a ring structure is used to derive the brightness bias for a shell, which is representative for the distribution of fluorophores of a VLP. Using Eq. B2c of the theory presented in (26) we arrive at a relative bias in brightness of $((1+8a^2/3)\sqrt{1+8a^2/3r})^{-1}-1$, where a is the dimensionless radius of the particle and r is the squared beam waist ratio as defined in (26). We experimentally determined $r=25$ from a fit of the autocorrelation function. VLPs with a diameter of 130 nm correspond to $a=0.15$, which leads to a brightness bias of -6%. In other words, the experimentally measured brightness underestimates the true brightness by 6%. This bias is negligible, because it is of the same order as the experimental uncertainty of the brightness measurement.

Some of our experiments used cells transfected with a plasmid mixture of labeled and unlabeled Gag. Transfection with a plasmid mixture potentially leads to a wide distribution of protein coexpression ratios, because of statistical effects of plasmid uptake by the cell. The magnitude of this statistical spread depends on the plasmid uptake. To characterize the size of this effect we carried out a study previously with dual-color detection on cells transfected with plasmid mixtures of cyan and yellow fluorescent protein (27). The cell-to-cell variations in protein coexpression ratio ranged from 20% to 50%. In addition, the analysis showed that the protein coexpression ratio exactly followed the plasmid ratio. Based on this result it seems reasonable that the coexpression ratio of labeled and unlabeled Gag is fairly constant from cell to cell. This expectation is further supported by PCH analysis, which recovers a single brightness species for the mixed VLP population. Thus, variations in labeled and unlabeled Gag expression must be small enough to be consistent with a single brightness description.

Previous studies suggested that labeling of Gag with fluorescent proteins interferes with the proper assembly of VLPs (28,29). However, TEM measurements showed no difference in the size distribution and shape of stained Gag and Gag^{YFP} VLPs. It was also reported previously that VLPs containing Gag^{GFP} appeared to create discontinuities in the observed thin-section EM, whereas coexpression of labeled and unlabeled Gag resulted in properly assembled particles (29). Thus, studying VLP properties as a function of their Gag/Gag^{YFP} composition provides a sensitive method of detecting interference of particle assembly by Gag^{YFP}. Autocorrelation analysis of mixed Gag/Gag^{YFP} VLPs showed that the average size of the mixed VLPs is independent of the Gag^{YFP} plasmid mole fraction. In addition, the Gag^{YFP} copy number of the mixed Gag/Gag^{YFP} VLPs scaled linearly with the Gag^{YFP} plasmid mole fraction. Taken together with the results of a biochemical experiment, wherein the relative amount of Gag and Gag^{YFP} present in mixed VLP samples was quantified on denaturing polyacrylamide gels, these studies show that the total copy number of labeled and unlabeled Gag remains the same for all VLPs regardless of their composition. The experiments also show that the Gag^{YFP} copy number measured by brightness directly reflects the mole fraction of labeled Gag, and support the conclusion that the Gag copy number is accurately determined by brightness. Interference with proper assembly should result in observable differences in the VLP composition as the mole fraction of labeled Gag approaches one. However, this behavior was not observed. Instead, all experimental results suggested that the composition of the VLP was not influenced by labeling and that experiments with labeled Gag reflect the properties of VLPs formed by unlabeled Gag (Figs. 4 and 5).

Accurate determination of the Gag copy number requires that the brightness of YFP is a stable quantity. As a first indication that YFP is a suitable fluorophore we verified that genetic tagging of YFP with a protein is not changing brightness (data not shown). We have also shown that the brightness of dimeric YFP doubles as compared to monomeric YFP (see Supporting Material), which shows the absence of quenching or dark states. Note that both fluorophores are in close enough proximity for homo-FRET to occur. But unlike hetero-FRET, homo-FRET does not change the brightness of the fluorophore. In addition, the fluorescence lifetime of YFP in VLPs is identical to YFP in solution, which excludes the presence of dynamic quenching. Additional support that self-quenching of YFP does not occur in VLPs is provided by the data in Fig. 4, which shows linear scaling of brightness with the mole-fraction of labeled Gag.

Each FFS experiment reports the properties of an ''ensemble of particles'' rather than a single particle, because the crossing of many different particles through the beam contributes to the collected fluorescence fluctuations. Ensemble measurements introduce population averaging, which reduces the ability to distinguish between closely related species. For example, a sample with a Gaussian distribution of particle sizes results in an autocorrelation function that is, within error, identical to the correlation function of single-sized particles. The particle diameter determined from the diffusion time of the correlation function equals the mean diameter of the Gaussian size distribution if all particles have the same brightness. If larger particles are brighter, then the diameter determined from the diffusion time is slightly skewed to a larger than average size.

This discussion is relevant, because it is known that the size distribution of the HIV-1 particles is heterogeneous. Cryoelectron microscopy (cryo-EM) showed particle sizes varying from 100 to over 200 nm, with an approximately Gaussian distribution (30). The mean diameter identified by the cryo-EM studies ranged from 130 to 150 nm. Our TEM experiments showed a mean particle diameter of 130 nm. This value agrees with the particle diameter determined from the autocorrelation function.

Similarly, particles with a narrow distribution of brightness values are described in FFS by a single averaged brightness species, whereas a broader distribution of brightness values would be identified as two or more discrete brightness species. Thus, the observation of two brightness species in some experiments most likely reflects the presence of a heterogeneous population of VLPs with a broad distribution of Gag copy numbers. By the same token, the data represented by a single brightness species most likely reflect a VLP sample with a narrower distribution of Gag copy numbers.

An intriguing finding of this study is the observation that the Gag stoichiometry of VLPs depends on sample preparation. Using different amounts of plasmid for transfection yielded VLPs with distinctly different stoichiometries. We observed copy numbers of Gag ranging from 750 to 2500. Our numbers overlap with earlier estimates of the Gag stoichiometry carried out on VLPs and virions (16–18,20,21). Our data suggest that the cellular concentration of Gag influences the stoichiometry. Higher amounts of plasmid used for transfection yield a higher concentration of Gag^{YFP} inside cells as judged from the fluorescence intensity, which correlates with an increase in the measured stoichiometry. Transient transfection results in a heterogeneous population of cells expressing Gag at different concentrations. Thus, such a cell population would produce VLPs with a heterogeneous Gag stoichiometry, as experimentally indicated by the presence of more than one brightness species. The lowest copy number reported by us is less than the smallest value (=1400) quoted by EM (21). We may speculate that cryo-EM studies use higher amounts of transfection agent, because of the need to produce high concentrations of particles, which according to our study favors higher Gag copy numbers. We tried to measure VLPs produced using higher transfection amounts than quoted in Table 1, but were unsuccessful because these samples contain large aggregated structures that get trapped in the laser beam. Because of

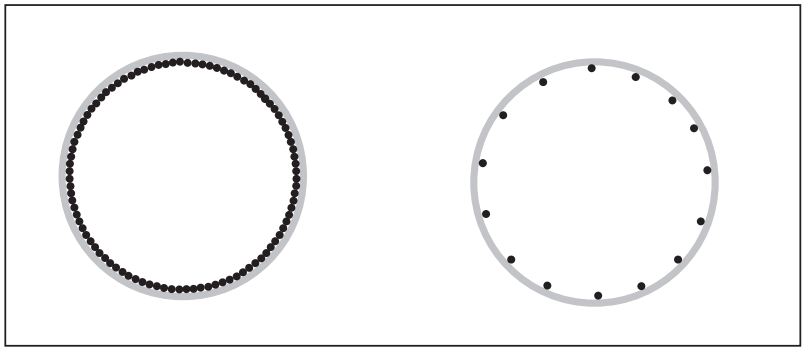

FIGURE 6 (*Left*) About 5000 copies of Gag protein are required to cover the surface area of a 140-nm particle. (*Right*) Our experimental data indicate that 750 copies of Gag protein are sufficient to form viral like particles, which corresponds to a surface coverage of ~15% as conceptually illustrated in the figure. For simplicity, evenly distributed Gag proteins are depicted. Recent data indicate that Gag proteins exist in patches (19).

this technical difficulty we are not able currently to explore the Gag copy number of VLPs at higher transfection amounts.

A higher Gag copy number (~5000) was obtained by a study of particles assembled in vitro (15). It is known that Gag assembles in solution into spherical shells with a size that matches VLPs produced by cells. Under in vitro conditions, self-assembly of Gag into particles is the only assembly mechanism available. The observed stoichiometry of 5000 Gag per particle agrees well with the expected copy number based on the known size of the Gag molecule and the surface area of the particle. Although geometrical constraints set an upper limit of ~5000 to the Gag copy number of VLPs, a recent study supports Gag stoichiometries of less than the maximum copy number, because discontinuities in the electron density along the membrane periphery of Gag bound to viral particles were observed by cryo-EM (19). It was estimated that, on average, only 40% of the viral surface is covered by a well-ordered Gag lattice. This study provides a structural model that is consistent with our brightness analysis.

The observation reported in this study that the Gag copy number varies, whereas the size of the VLPs stays the same, argues that self-assembly of Gag into a closed shell is not a required mechanism for VLP assembly in cells. Our observations imply that cells (i.e., cellular proteins or factors) play an important role in determining the stoichiometry of VLPs. It is known that Gag interacts with a number of cellular proteins and lipids, which are involved in the budding of particles (31). However, the role these cellular factors play in the assembly process of the virus remains an evolving story and requires further experimental characterization (32,33).

No brightness heterogeneity was detectable for the lowest amount of transfected plasmid (Table 1). This experiment also yielded the lowest observed Gag copy number. Further reduction of the transfected DNA resulted in very few VLPs and could not be measured. Taken together, these data suggest that a minimum Gag copy number is required for VLP production by cells. In this study, a minimum copy number of 750 was observed. Under these conditions, only 15% of the lipid surface area is covered with Gag protein (Fig. 6). Interestingly, it was experimentally estimated that the core of the mature virion contains ~1000-1500 capsid proteins (34,35), whereas theoretical models predict core formation with as little as 420 capsid proteins (36). Because cleavage of each Gag molecule during the maturation process of the virus yields one capsid protein, the Gag stoichiometries observed here would yield a sufficient number of capsid proteins for core formation. Thus, from a biological point of view the observed Gag copy numbers suffice for the formation of infectious virions from immature particles.

CONCLUSIONS

In this study, brightness analysis has been extended to large structures containing thousands of proteins. We successfully showed that brightness is a measure of stoichiometry, as illustrated by the linear relationship between brightness and the mole fraction of labeled Gag proteins in VLPs. Our data show that VLPs are successfully produced in COS-1 cells over a wide range of HIV-1 Gag stoichiometries. The size of the VLPs remained unchanged despite variations in the Gag copy number. This observation shows that large areas of the VLP membrane are void of Gag protein. Therefore, self-assembly of Gag into an enveloping protein shell is not required for VLP formation by cells. Other factors, such as protein and membrane interactions, are likely to contribute significantly to the assembly of VLPs. Our results suggest that the cellular Gag concentration is one of the factors influencing the stoichiometry of Gag within the VLP. We showed that changes in sample preparation resulted in VLPs with different Gag copy numbers. This observation offers a potential explanation for the differences in the Gag copy number reported in the literature. By analyzing mixed Gag/Gag^{YFP} VLPs, we showed that fluorescent labeling of Gag does not influence the properties of the particle. Our results illustrate that FFS provides information about the composition of particles that is difficult to obtain by other methods. For example, a potential application of FFS is the characterization of the amount of proteins carried by vesicles. In summary, FFS promises to provide unique contributions to the understanding of viral particles and other complex structures.

SUPPORTING MATERIAL

Two tables are available at http://www.biophysj.org/biophysj/supplemental/S0006-3495(09)00020-4.

We thank Dr. Paul Spearman (Emory University) for providing the Gag-YFP plasmid.

This work was supported by grants from the National Institutes of Health (GM64589 to J.D.M, GM065056 to K.M.-F. and AI57735 to L.M.M) and the National Science Foundation (PHY-0346782 to J.D.M.).

REFERENCES

1. Thompson, N. L., A. M. Lieto, and N. W. Allen. 2002. Recent advances in fluorescence correlation spectroscopy. *Curr. Opin. Struct. Biol.* 12:634–641.
2. Magde, D., E. Elson, and W. W. Webb. 1972. Thermodynamic fluctuations in a reacting system: measurement by fluorescence correlation spectroscopy. *Phys. Rev. Lett.* 29:705–708.
3. Chen, Y., J. D. Müller, P. T. C. So, and E. Gratton. 1999. The photon counting histogram in fluorescence fluctuation spectroscopy. *Biophys. J.* 77:553–567.
4. Berland, K. M. 2004. Fluorescence correlation spectroscopy: a new tool for quantification of molecular interactions. *Methods Mol. Biol.* 261:383–398.
5. Hwang, L. C., and T. Wohland. 2007. Recent advances in fluorescence cross-correlation spectroscopy. *Cell Biochem. Biophys.* 49:1–13.
6. Kohl, T., and P. Schwille. 2005. Fluorescence correlation spectroscopy with autofluorescent proteins. *Adv. Biochem. Eng. Biotechnol.* 95: 107–142.
7. Kolin, D. L., and P. W. Wiseman. 2007. Advances in image correlation spectroscopy: measuring number densities, aggregation states, and dynamics of fluorescently labeled macromolecules in cells. *Cell Biochem. Biophys.* 49:141–164.
8. Saffarian, S., Y. Li, E. L. Elson, and L. J. Pike. 2007. Oligomerization of the EGF receptor investigated by live cell fluorescence intensity distribution analysis. *Biophys. J.* 93:1021–1031.
9. Thompson, N. L., and B. L. Steele. 2007. Total internal reflection with fluorescence correlation spectroscopy. *Nat. Protocols.* 2:878–890.
10. Chen, Y., L. N. Wei, and J. D. Müller. 2003. Probing protein oligomerization in living cells with fluorescence fluctuation spectroscopy. *Proc. Natl. Acad. Sci. USA.* 100:15492–15497.
11. Chen, Y., and J. D. Müller. 2007. Determining the stoichiometry of protein hetero-complexes in living cells with fluorescence fluctuation spectroscopy. *Proc. Natl. Acad. Sci. USA.* 104:3147–3152.
12. Chen, Y., L. N. Wei, and J. D. Müller. 2005. Unraveling protein-protein interactions in living cells with fluorescence fluctuation brightness analysis. *Biophys. J.* 88:4366–4377.
13. Gheysen, D., E. Jacobs, F. de Foresta, C. Thiriart, M. Francotte, et al. 1989. Assembly and release of HIV-1 precursor Pr55gag virus-like particles from recombinant baculovirus-infected insect cells. *Cell.* 59:103–112.
14. Karacostas, V., K. Nagashima, M. A. Gonda, and B. Moss. 1989. Human immunodeficiency virus-like particles produced by a vaccinia virus expression vector. *Proc. Natl. Acad. Sci. USA.* 86:8964–8967.
15. Briggs, J. A., M. N. Simon, I. Gross, H. G. Krausslich, S. D. Fuller, et al. 2004. The stoichiometry of Gag protein in HIV-1. *Nat. Struct. Mol. Biol.* 11:672–675.
16. Layne, S. P., M. J. Merges, M. Dembo, J. L. Spouge, S. R. Conley, et al. 1992. Factors underlying spontaneous inactivation and susceptibility to neutralization of human immunodeficiency virus. *Virology.* 189: 695–714.
17. Piatak, M., Jr., M. S. Saag, L. C. Yang, S. J. Clark, J. C. Kappes, et al. 1993. High levels of HIV-1 in plasma during all stages of infection determined by competitive PCR. *Science.* 259:1749–1754.
18. Vogt, V. M., and M. N. Simon. 1999. Mass determination of Rous sarcoma virus virions by scanning transmission electron microscopy. *J. Virol.* 73:7050–7055.
19. Wright, E. R., J. B. Schooler, H. J. Ding, C. Kieffer, C. Fillmore, et al. 2007. Electron cryotomography of immature HIV-1 virions reveals the structure of the CA and SP1 Gag shells. *EMBO J.* 26:2218–2226.
20. Yeager, M., E. M. Wilson-Kubalek, S. G. Weiner, P. O. Brown, and A. Rein. 1998. Supramolecular organization of immature and mature murine leukemia virus revealed by electron cryo-microscopy: implications for retroviral assembly mechanisms. *Proc. Natl. Acad. Sci. USA.* 95:7299–7304.
21. Zhu, P., E. Chertova, J. Bess, Jr., J. D. Lifson, L. O. Arthur, et al. 2003. Electron tomography analysis of envelope glycoprotein trimers on HIV and simian immunodeficiency virus virions. *Proc. Natl. Acad. Sci. USA.* 100:15812–15817.
22. Derdowski, A., L. Ding, and P. Spearman. 2004. A novel fluorescence resonance energy transfer assay demonstrates that the human immunodeficiency virus type 1 Pr55Gag I domain mediates Gag-Gag interactions. *J. Virol.* 78:1230–1242.
23. Hillesheim, L. N., and J. D. Müller. 2003. The photon counting histogram in fluorescence fluctuation spectroscopy with non-ideal photodetectors. *Biophys. J.* 85:1948–1958.
24. Müller, J. D., Y. Chen, and E. Gratton. 2000. Resolving heterogeneity on the single molecular level with the photon counting histogram. *Biophys. J.* 78:474–486.
25. Doultree, J. C., R. E. Kiernan, J. Y. Lee, D. S. Bowden, D. A. McPhee, et al. 1992. A new electron microscope positive staining method for viruses in suspension. *J. Virol. Methods.* 37:321–335.
26. Wu, B., Y. Chen, and J. D. Muller. 2008. Fluorescence correlation spectroscopy of finite-sized particles. *Biophys. J.* 94:2800–2808.
27. Olmstead, S. 2004. Study of cotransfection and coexpression in cells. MS thesis. University of Minnesota/Twin Cities.
28. Larson, D. R., M. C. Johnson, W. W. Webb, and V. M. Vogt. 2005. Visualization of retrovirus budding with correlated light and electron microscopy. *Proc. Natl. Acad. Sci. USA.* 102:15453–15458.
29. Pornillos, O., D. S. Higginson, K. M. Stray, R. D. Fisher, J. E. Garrus, et al. 2003. HIV Gag mimics the Tsg101-recruiting activity of the human Hrs protein. *J. Cell Biol.* 162:425–434.
30. Fuller, S. D., T. Wilk, B. E. Gowen, H. G. Krausslich, and V. M. Vogt. 1997. Cryo-electron microscopy reveals ordered domains in the immature HIV-1 particle. *Curr. Biol.* 7:729–738.
31. Resh, M. D. 2005. Intracellular trafficking of HIV-1 Gag: how Gag interacts with cell membranes and makes viral particles. *AIDS Rev.* 7:84–91.
32. Demirov, D. G., and E. O. Freed. 2004. Retrovirus budding. *Virus Res.* 106:87–102.
33. Yap, M. W., and J. P. Stoye. 2003. Bending out and breaking away: host-cell accomplices in retroviral escape. *J. Biol.* 3:3.
34. Briggs, J. A., T. Wilk, R. Welker, H. G. Krausslich, and S. D. Fuller. 2003. Structural organization of authentic, mature HIV-1 virions and cores. *EMBO J.* 22:1707–1715.
35. Li, S., C. P. Hill, W. I. Sundquist, and J. T. Finch. 2000. Image reconstructions of helical assemblies of the HIV-1 CA protein. *Nature.* 407:409–413.
36. Nguyen, T. T., R. F. Bruinsma, and W. M. Gelbart. 2006. Continuum theory of retroviral capsids. *Phys. Rev. Lett.* 96:078102.